npg

ORIGINAL ARTICLE

Isotope array analysis of *Rhodocyclales* uncovers functional redundancy and versatility in an activated sludge

Martin Hesselsoe[1], Stephanie Füreder[2], Michael Schloter[3], Levente Bodrossy[4], Niels Iversen[1], Peter Roslev[1], Per Halkjær Nielsen[1], Michael Wagner[2] and Alexander Loy[2]

[1]*Department of Biotechnology, Chemistry and Environmental Engineering, Aalborg University, Aalborg, Denmark;* [2]*Department of Microbial Ecology, University of Vienna, Wien, Austria;* [3]*Department of Terrestrial Ecogenetics, Helmholtz Zentrum München—National Research Center for Environmental Health, Neuherberg, Germany and* [4]*Department of Bioresources/Microbiology, ARC Seibersdorf Research GmbH, Seibersdorf, Austria*

Extensive physiological analyses of different microbial community members in many samples are difficult because of the restricted number of target populations that can be investigated in reasonable time by standard substrate-mediated isotope-labeling techniques. The diversity and ecophysiology of *Rhodocyclales* in activated sludge from a full-scale wastewater treatment plant were analyzed following a holistic strategy based on the isotope array approach, which allows for a parallel functional probing of different phylogenetic groups. Initial diagnostic microarray, comparative 16S rRNA gene sequence, and quantitative fluorescence *in situ* hybridization surveys indicated the presence of a diverse community, consisting of an estimated number of 27 operational taxonomic units that grouped in at least seven main *Rhodocyclales* lineages. Substrate utilization profiles of probe-defined populations were determined by radioactive isotope array analysis and microautoradiography-fluorescence *in situ* hybridization of activated sludge samples that were briefly exposed to different substrates under oxic and anoxic, nitrate-reducing conditions. Most detected *Rhodocyclales* groups were actively involved in nitrogen transformation, but varied in their consumption of propionate, butyrate, or toluene, and thus in their ability to use different carbon sources in activated sludge. This indicates that the functional redundancy of nitrate reduction and the functional versatility of substrate usage are important factors governing niche overlap and differentiation of diverse *Rhodocyclales* members in this activated sludge.

Introduction

Many members of the betaproteobacterial order *Rhodocyclales* are widespread and abundant in wastewater treatment systems (Juretschko *et al.*, 2002; Etchebehere *et al.*, 2003; Tsuneda *et al.*, 2005; Liu *et al.*, 2006), and have diverse physiological capabilities that are beneficial for the degradation and transformation of pollutants, such as nitrogen, phosphorous, and aromatic compounds (Loy *et al.*, 2005). For example, yet uncultivated 'Candidatus Accumulibacter' species are involved

in phosphorus removal from wastewater (Hesselmann *et al.*, 1999; Crocetti *et al.*, 2000). In addition, anaerobic nitrogen removal by denitrification in full- and laboratory-scale wastewater treatment systems is predominantly catalyzed by 'Candidatus Accumulibacter'-, *Dechloromonas*-, *Thauera*- and *Azoarcus*-related bacteria, as recently shown by stable isotope probing and fluorescence *in situ* hybridization coupled with microautoradiography (MAR-FISH) studies (Kong *et al.*, 2004; Ginige *et al.*, 2005; Thomsen *et al.*, 2007; Morgan-Sagastume *et al.*, 2008). Some members of the *Rhodocyclales* are endowed with additional catabolic capabilities of potential benefit for wastewater treatment. Certain *Thauera* and *Dechloromonas* strains degrade oil derivates such as toluene (Shinoda *et al.*, 2004; Chakraborty *et al.*, 2005), and might thus contribute

1350

to reducing the ecological burden of such aromatic waste compounds. However, niche partitioning of different, co-occurring *Rhodocyclales* species in activated sludge and the implication of this diversity for the functioning and stability of the wastewater treatment process is still poorly understood.

The vast majority of microorganisms that are responsible for central functions in many natural and biotechnological ecosystems (such as wastewater treatment plants) have not yet been cultured. Radioactive- and stable-isotope-substrate-mediated labeling methods for linking the identity of an uncultivated microorganism with its physiological abilities have thus become indispensable for our understanding of microbial ecology and ecosystem function. Stable isotope probing of nucleic acids (Radajewski *et al.*, 2000; Manefield *et al.*, 2002) and MAR-FISH (Lee *et al.*, 1999; Ouverney and Fuhrman, 1999) represent the core of our methods arsenal for structure–function analysis of complex microbial communities (reviewed in Friedrich, 2006; Madsen, 2006; Wagner *et al.*, 2006; Whiteley *et al.*, 2006; Neufeld *et al.*, 2007). Additional methods were recently developed on the basis of advanced secondary ion mass spectrometry (SIMS) and vibrational spectroscopy techniques and their adaptation for measurements in biological systems. The combination of multi-isotope imaging mass spectrometry (also called nanoSIMS) (Behrens *et al.*, 2008; Li *et al.*, 2008; Musat *et al.*, 2008) or Raman microspectroscopy (Huang *et al.*, 2007) with FISH offers unprecedented opportunities for tracing substrate incorporation at the (sub)cellular level (Wagner, 2009). Each of these isotope techniques has its specific advantages and disadvantages (Wagner *et al.*, 2006; Neufeld *et al.*, 2007), but all are limited by the number of samples and/or microbial groups that can be analyzed with justifiable effort. DNA microarrays containing hundreds to thousands of nucleic acid probes are suited for high-throughput analyses. The application of rRNA-targeted oligonucleotide microarrays (PhyloChips) for microbial community analysis (Liu *et al.*, 2001; Loy *et al.*, 2002; Wilson *et al.*, 2002; Zhou, 2003; Bodrossy and Sessitsch, 2004; Lehner *et al.*, 2005; Loy and Bodrossy, 2006; Palmer *et al.*, 2006) has propelled the development of the so-called isotope array technique, which allows the parallel identification and functional screening of numerous phylogenetic groups of microorganisms for their ability to consume a radioactive substrate (Adamczyk *et al.*, 2003). In a first proof-of-principle study, a manually spotted prototype microarray consisting of six rRNA-targeted oligonucleotide probes was employed for isotope array surveys of ammonia-oxidizing bacteria in activated sludge samples (Adamczyk *et al.*, 2003). However, the applicability of PhyloChips containing larger probe sets and produced with automatic spotting devices for the detection of fluorescently and radioactively labeled native rRNA remains to be proven.

The main objectives of this study were to adapt the isotope array technique for PhyloChips containing a larger number of probes and to use it for insights into the substrate-consumption profiles of *Rhodocyclales* in activated sludge incubated under oxic and anoxic, nitrate-reducing conditions. For this purpose, a recently designed 16S rRNA-targeted microarray, consisting of 79 nested oligonucleotide probes, for most cultivated and uncultivated *Rhodocyclales* (RHC-PhyloChip) (Loy *et al.*, 2005) was used. Microarray results were complemented by retrieval and phylogenetic analyses of 16S rRNA gene sequences, and by using existing and newly developed *Rhodocyclales* subgroup-specific probes for quantitative FISH and MAR-FISH analyses.

Materials and methods

Sampling of activated sludge
Activated sludge samples were collected in October 2004 at the municipal wastewater treatment plant, Aalborg East (Denmark, 100 000 person equivalents). Nitrogen and phosphorus in the plant are removed biologically by a Biodenipho configuration in which influent is mixed with activated sludge in anaerobic tanks before entering tanks with alternating denitrifying and nitrifying conditions. Samples for this study were collected in the denitrifying–nitrifying tanks. Samples for isotope labeling and DNA extraction were stored at $5\,^{\circ}C$ in the dark (for not more than 3 days) and at $-20\,^{\circ}C$, respectively. For FISH analyses, activated sludge was fixed with paraformaldehyde as described earlier (Daims *et al.*, 2005).

DNA extraction
Genomic DNA was isolated from activated sludge samples by using the Power Soil DNA Kit (MoBio Laboratories Inc., Carlsbad, CA, USA) according to the manufacturer's instructions; with the exception that in the final step DNA was eluted from the column with $2 \times 30\,\mu l$ of double-distilled water.

PCR amplification of 16S rRNA genes
Amplification of 16S rRNA gene fragments from DNA of the activated sludge sample was performed by using the bacterial primer pairs 616V-630R and 616V-1492R, and the *Rhodocyclales* subgroup-selective primer pairs A, R or Z, together targeting almost all *Rhodocyclales* (Loy *et al.*, 2005).

Isotope labeling of activated sludge
Activated sludge was diluted 1:1 with HEPES [*N*-(2-hydroxyethyl) piperazine-*N'*-2-ethanesulfonic acid]-buffered liquid mineral medium without ammonia (Aakra *et al.*, 2000) to a final concentration of 2 g suspended solids per liter. Subsequently, the diluted sludge was flushed for 1 hour with CO_2-free air to reduce dissolved inorganic carbon. This treatment

decreased the concentration of dissolved inorganic carbon from 4 to 1 mM as measured by gas chromatography after acidification of subsamples (Chai et al., 2001). After aeration, 1 mM ammonium was added to all samples to avoid nitrogen limitation. Sludge samples were additionally incubated with 5 mg of allylthiourea per liter to inhibit assimilation of CO_2 by autotrophic ammonia-oxidizing bacteria (Bedard and Knowles, 1989). For anoxic incubations, sludge samples were vacuum flushed with N_2 immediately before and during the addition of radioactive compounds. Heterotrophic $^{14}CO_2$ assimilation (Roslev et al., 2004; Hesselsoe et al., 2005) was exploited for radioactive labeling of biomass by adding $NaH^{14}CO_3$ (58 mCi mmol^{-1}, Amersham Pharmacia Biotech, Buckinghamshire, UK) to 10 ml aliquots of diluted sludge in 60 ml glass vials (final concentration was in the range of 60–100 μCi ml^{-1}). Subsequently, different unlabeled electron donors (5 mM propionate, 5 mM butyrate or 10 mg l^{-1} toluene) were added. Control incubations devoid of added electron donors were included to monitor and quantify background assimilation of $^{14}CO_2$ in the absence of added organic substrates. Furthermore, additional activated sludge samples were incubated with 0.17 mM [^{14}C]propionate {[1-^{14}C] propionic acid sodium salt (56.7 mCi mmol^{-1}), MP Biomedicals Inc., Solon, OH, USA} (final concentration 10 μCi ml^{-1}) and with 2 mM unlabeled propionate to avoid substrate limitation during the incubation (ratio of ^{14}C-labeled to unlabeled propionate was 1:11.8). All sludge slurries were exposed to atmospheric oxygen or 2 mM nitrate, sealed with gas-tight rubber stoppers, and incubated at room temperature in the dark for 4.5 h (propionate and butyrate) or 24 h (toluene).

Incorporation of ^{14}C into biomass was monitored during the incubations. For this purpose, subsamples (20–100 μl aliquots) were harvested with a syringe, filtered through a 0.2-μm-pore-sized mixed-cellulose filter (Advantec MFS Inc., Pleasanton, CA, USA), acidified, dissolved in scintillation fluid, and quantified by liquid scintillation counting as described earlier (Hesselsoe et al., 2005).

After incubation, 90% (v/v) of the biomass from each vial was harvested by centrifugation, resuspended in RNAlater (Ambion, Austin, TX, USA), cooled at 4 °C during the transport between laboratories, and finally stored at −20 °C until RNA extraction. The remaining 10% (v/v) of the biomass was fixed with paraformaldehyde for MAR-FISH analysis.

In vitro transcription of 16S rRNA
All experimental steps involving RNA were carried out under RNase-free conditions (Sambrook and Russell, 2001). Fluorescently labeled in vitro-transcribed RNA was used for optimizing RHC-Phylo-Chip hybridization conditions. For subsequent in vitro transcription, the 16S rRNA gene from

activated sludge clone S3 (AF072918) was amplified by PCR using the general bacterial primers T3-BACT8F (5′-**AATTAACCCTCACTAAAGGG**AGAGT TTGATYMTGGCTC-3′, the T3 promoter sequence is depicted in bold) and 630R (Loy et al., 2002) and subsequently purified by using the QIAquick PCR purification kit (Qiagen, Wien, Austria). Reaction mixtures (30 μl) for in vitro transcription were prepared in T3 RNA polymerase transcription buffer (Fermentas, St Leon-Rot, Germany), contained 0.5–1 μg purified PCR product, 1 mM of each ribonucleotide, 20 U RNasin and 60 U of T3 RNA polymerase (Fermentas), and were incubated at 37 °C for 4 h. In the next step, the DNA template was digested by adding 3 μl of DNase I buffer and 3 U of RNase-free DNase I (Fermentas) to the reaction mixture and incubation at 37 °C for 15 min. The 16S rRNA was subsequently purified using the RNeasy MinElute Clean-up Kit (Qiagen). Quality and concentration of RNA were determined by agarose gel electrophoresis and spectrophotometric analysis (Adamczyk et al., 2003).

RNA extraction
RNA extraction from activated sludge stored in RNAlater was essentially carried out as described earlier (Adamczyk et al., 2003). The extracted RNA was additionally purified using filter cartridges and solutions that were supplied with the RiboPure-Bacteria or RNAqueous RNA extraction kits (Ambion). Agarose gel electrophoresis showed that the filter cartridge purification removed all small RNA fragments without substantial loss of intact small- and large-subunit rRNA. A total of 5–7 μg of RNA was obtained from 1 ml of undiluted activated sludge.

Spotting of DNA microarrays
Characteristics of oligonucleotide probes used for the production of the RHC-PhyloChips were described earlier (Loy et al., 2005) and can be viewed at probeBase (http://www.microbial-ecology.net/probebase/) (Loy et al., 2007), including the theoretical binding affinity of each probe to its perfectly matched rRNA, calculated as free energy ΔG_{12} (Yilmaz and Noguera, 2004). A 384-well flat bottom plate was prepared with 30 μl of 50 pmol μl^{-1} oligonucleotide solutions in 50% dimethyl sulfoxide. Probes were printed with a single pin on aldehyde group-coated CSS-100 glass slides (CEL Associates, Houston, TX, USA) with an OmniGrid 100 spotter (Genomics Solutions, Ann Arbor, MI, USA) at 50% relative humidity and 22 °C. RHC-PhyloChips for hybridization of labeled PCR products were spotted with a SMP3 pin (tip diameter 100 μm, TeleChem International Inc., Sunnyvale, CA, USA) in triplicate on each slide. In contrast, RHC-PhyloChips for isotope array analysis were spotted with a SMP15XB pin (tip diameter 600 μm, TeleChem) in duplicate on

each slide. Spotted slides were further processed as described earlier (Loy *et al.*, 2002). The first and last slides from each spotting run were hybridized with a fluorescently labeled 16S rRNA gene PCR product from *Desulfovibrio halophilus* (DSM 5663) to confirm the quality of the spotting. Slides were stored in the dark for <3 months before use.

Fluorescence labeling and microarray hybridization

Fluorescence labeling of PCR products and hybridization on microarrays were performed as outlined earlier (Loy *et al.*, 2002). Per RHC-PhyloChip hybridization, two times 300 ng of purified 16S rRNA gene PCR product were random prime labeled in separate reactions and pooled before microarray hybridization to ameliorate labeling biases.

For fluorescence labeling of RNA, a direct chemical labeling procedure was performed using the CyScribe Direct mRNA labeling Kit (Amersham Bioscience, Uppsala, Sweden) as described earlier (Adamczyk *et al.*, 2003). Only one type of dye (Cy3 or Cy5) was used for a coherent set of experiments. Before hybridization, the RNA was fragmented for 30 min at 60 °C in a solution containing 0.2 M Tris-HCl (pH 7.4) and 0.01 $ZnSO_4$. After fragmentation, the solution was immediately chilled on ice, and 0.05 M EDTA was added to deactivate Zn^{2+} and stop the fragmentation process. RNasin was added to a final concentration of 1 U μl^{-1}. Subsequently, fluorescently labeled and fragmented RNA was divided in aliquots and stored at −20 °C until hybridization. Microarray hybridization of RNA was performed as described earlier (Adamczyk *et al.*, 2003). The quantity of RNA and percentage of formamide in the hybridization reaction was varied during optimization of the hybridization procedure.

Fluorescence scanning

Fluorescence images of the RHC-PhyloChip were recorded by scanning the slides with a GenePix Personal 4100A array scanner (Axon Instruments, Molecular Devices Corporation, Sunnyvale, CA, USA). The fluorescent signals were quantified by using the GenePix Pro software version 5.1 (Axon Instruments). Slides hybridized with fluorescently labeled PCR products were analyzed as described earlier (Loy *et al.*, 2005). When analyzing microarrays hybridized with RNA, all slides in an experiment were scanned at the same laser intensity and the same amplification gain of the photomultiplier tube to ensure slide-to-slide comparability. For subsequent calculation of the cumulative fluorescence intensities, the scanned images did not contain signal-saturated pixels in the probe spot and background area. During image analysis, the circles defining the individual probe spots were adjusted to cover the whole spot area. Before the calculation of the cumulative fluorescence intensity of a probe spot, the mean pixel intensity in the local

background was subtracted from the intensity measured for each pixel in the spot.

Radioactivity scanning and calculation of activity values

Radioactivity was recorded with a β-imager (Bio-Space Mesures, Paris, France) using a highly sensitive scintillation membrane (Zinsser Analytics, Frankfurt, Germany) and chemoluminescence detection. To obtain an optimal signal-to-noise ratio the slides were incubated for 24 h. The radioactivity for each spot and background was quantified in disintegrations per minute using β-Vision software (BioSpace Mesures). In analogy to the fluorescence image analysis, the circles defining the individual probe spots were adjusted to cover the whole spot area before measuring the background-corrected cumulative radioactivity. The activity value (*A*-value) of each probe spot was calculated as the ratio of the cumulative radioactive intensity and the cumulative fluorescence intensity (Adamczyk *et al.*, 2003).

Cloning and comparative sequence analysis

The 16S rRNA gene sequences of *Rhodocyclales* were retrieved from the pristine-activated sludge sample and phylogenetically analyzed as described earlier (Loy *et al.*, 2005). In brief, PCR products obtained with the primer pairs A, R and Z were used for the construction of three separate 16S rRNA gene clone libraries and insert sequences of the isolated plasmids were sequenced using the vector-targeted primers M13F and M13R. Chimeric and *Rhodocylales* sequences were identified by employing the respective software tools of the Ribosomal Database Project II website (Cole *et al.*, 2005) and by phylogenetic analyses with the ARB program package (Ludwig *et al.*, 2004). Homologous coverage C was calculated according to $C = [1-(n_1 \times N^{-1})] \times 100\%$, with n_1 as number of operational taxonomic units (OTUs) containing only one sequence, and N as total number of clones analyzed. Non-parametric Chao1 richness estimates were calculated by using the program EstimateS (version 7.00, http://viceroy.eeb.uconn.edu/estimates). The presence of fully complementary target sites for RHC-PhyloChip probes in the retrieved 16S rRNA sequences were analyzed by using the 'Probe Match' option of ARB and the program CalcOligo 2.03 (Stralis-Pavese *et al.*, 2004).

In silico *probe design and evaluation*

Novel 16S rRNA-targeted oligonucleotide probes for FISH (Table 1), specific for selected *Rhodocyclales*-Aalborg East activated sludge clones, were designed by using the 'Design Probes' option of ARB and evaluated with probeCheck (Loy *et al.*, 2008). Final probes contained a maximal number of strongly destabilizing

Table 1 rRNA-targeted oligonucleotide probes used for FISH

Name	Full name[a]	Sequence 5′–3′	Formamide (%)	Specificity[b]	Reference
EUB338[c]	S-D-Bact-0338-a-A-18	GCTGCCTCCCGTAGGAGT	0–50	Most *bacteria*	Amann *et al.* (1990)
EUB338-II[c]	S-*-BactP-0338-a-A-18	GCAGCCACCCGTAGGTGT	0–50	*Planctomycetes*	Daims *et al.* (1999)
EUB338-III[c]	S-*-BactV-0338-a-A-18	GCTGCCACCCGTAGGTGT	0–50	*Verrucomirobia*	Daims *et al.* (1999)
BET42a[d]	L-C-bProt-1027-a-A-17	GCCTTCCCACTTCGTTT	35	*Betaproteobacteria*	Manz *et al.* (1992)
AT1458	S-*-AT-1459-a-A-21	GAATCTCACCGTGGTAAGCGC	50	Most members of the *Azoarcus–Thauera–Denitromonas* lineage	Rabus *et al.* (1999)
PAO651[e]	S-G-Accba-0651-a-A-18	CCCTCTGCCAAACTCCAG	35	Most members of the 'Candidatus Accumulibacter' cluster, activated sludge clones R2, R8	Crocetti *et al.* (2000)
RHC439[e]	S-*-RHC-0439-a-A-18	CNATTTCTTCCCCGCCGA	30	*Rhodocyclus* species, most member of the 'Candidatus Accumulibacter' cluster, *Azospira* lineage, activated sludge clones R2, R3, R7, R8 and R9	Hesselmann *et al.* (1999)
RHC445[f]	S-*-RHC-0445-a-A-18	CCCATGCGATTTCTTCCC	20–30	Activated sludge clones R10, R11, *Dechloromonas denitrificans*	This study
RHC827[f]	S-*-RHC-0827-a-A-18	TTACCCACCCAACACCTA	20–30	Activated sludge clones R10, R11, *Dechloromonas denitrificans*	This study
ZOGLO1416	S-G-Zoglo-1416-a-A-20 (S-*-OTU1-1415-a-A-20)	TTCTGGTAAACCCCACTCCC	25	Genus *Zoogloea*	Juretschko *et al.* (2002)
ZOGLO454	S-*-Zoglo-0454-a-A-18	GGGTATTCACCGATGCGT	25	Activated sludge *Zoogloea* clones Z2, Z4, Z6, Z12	This study
ZORAM441	S-S-Zoram-0441-a-A-18	TGCGATTTCTTTCCACCT	25	*Zoogloea ramigera*, activated sludge clones Z7, Z8, Z10, Z11	This study

[a]rRNA-targeted probe nomenclature according to Alm *et al.* (1996).
[b]The *in silico* coverage and specificity of the probes can be re-evaluated with probeCheck (Loy *et al.*, 2008).
[c]EUB338, EUB338-II and EUB338-III were applied simultaneously to target most bacteria (Daims *et al.*, 1999).
[d]BET42a was used together with the unlabeled competitor GAM42a (5′-GCCTTCCCACATCGTTT-3′).
[e]PAO651 and RHC439, each labeled with a different fluorescent dye, were used simultaneously. Cells, represented by clones R2 and R8, showed signals with both probes, whereas cells represented by clones R3, R7, showed signals only with RHC439.
[f]RHC445 and RHC827, each labeled with a different fluorescent dye, were used simultaneously to enhance specific detection of clones R10 and R11.

mismatching bases that were centrally located in the probe-binding sites of non-target sequences.

Quantitative FISH and MAR-FISH
The abundance of selected *Rhodocyclales* groups in the activated sludge sample was determined by FISH with confocal laser scanning microscopy and subsequent image analysis by using the DAIME program version 1.1 (Daims *et al.*, 2006). Ribosomal RNA-targeted oligonucleotide probes that were used for FISH are depicted in Table 1. Optimal hybridization conditions for newly developed probes were determined as outlined earlier (Juretschko *et al.*, 2002). Further details on the probes can be found at probeBase (Loy *et al.*, 2007). In addition, the incorporation of radioactive substrate into activated sludge bacteria was monitored on a single-cell level by using MAR-FISH (Lee *et al.*, 1999).

Nucleotide sequence accession numbers
The sequences determined in this study were deposited at the EMBL Nucleotide Sequence Database under accession numbers AM268340 to AM268373.

Results

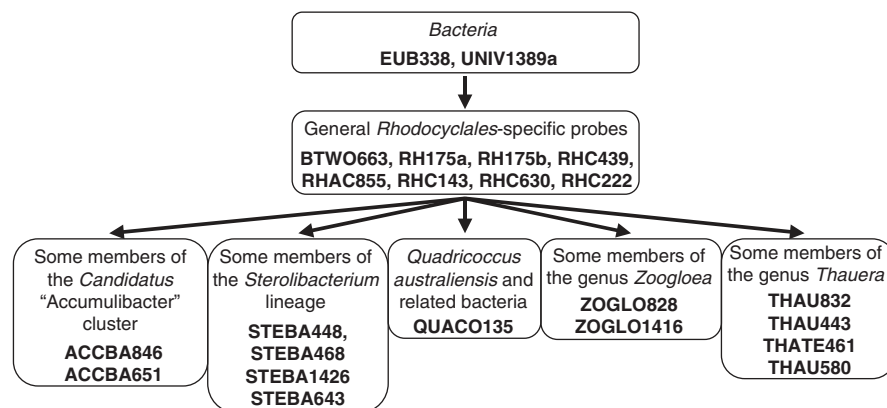Rhodocyclales *diversity in Aalborg East activated sludge*
The presence and abundance of members of the order *Rhodocyclales* in a nitrifying–denitrifying, phosphorus-removing activated sludge were analyzed by applying different molecular methods. Initially, 16S rRNA genes were amplified from activated sludge DNA by using general bacterial and *Rhodocyclales* group-selective primers. PCR products were obtained with all primers, except with the *Zoogloea*-selective Z primer pair. A PCR product was only obtained with the Z primer pair by applying a nested PCR approach in which 1 μl of the bacterial 16S rRNA gene PCR product served as template. The different PCR products were fluorescently labeled in separate reactions and subsequently hybridized individually with RHC-PhyloChips. Based on positive probe signals, a

composite microarray fingerprint of the *Rhodocyclales* community present in the activated sludge was created by merging the separate microarray hybridization patterns obtained with the *Rhodocyclales* subgroup selective and the common bacterial 16S rRNA gene PCR products (Loy *et al.*, 2005). This merged microarray pattern indicated the presence of bacteria belonging or related to the *Sterolibacterium* lineage, the 'Candidatus Accumulibacter' cluster, and the genera *Quadricoccus*, *Thauera* and *Zoogloea* (Figure 1).

In the following step, microarray results were evaluated and the phylogeny of *Rhodocyclales* present in the Aalborg East wastewater treatment plant was further resolved by PCR amplification of their 16S rRNA genes using the subgroup-selective primers, cloning, and subsequent sequencing. Only sequences affiliated with the order *Rhodocylales* were further analyzed. After removal of chimeras, the remaining 34 sequences were grouped in 16 OTUs using an arbitrary 16S rRNA sequence similarity threshold of 97%. Calculation of the homologous coverage indicated that 77% of the OTU diversity in the combined gene libraries was sampled. Based on Chao1 analysis, 27 OTUs of *Rhodocyclales* were indicated. Phylogenetic analysis of the clone sequences confirmed presence of members of the *Sterolibacterium* lineage and the genera 'Candidatus Accumulibacter', *Thauera* and *Zoogloea*, as indicated by the RHC-PhyloChip fingerprint (Figure 2). In addition, some of the sequences affiliated with these taxa contained the fully complementary target sites for those probes that were positive in the microarray analyses (Figure 3). The positive signal of RHC-PhyloChip probe QUACO135, indicating the presence of *Quadricoccus australiensis* and related bacteria (Figure 1), most likely derive from bacteria represented by clones R10 and R11, which were retrieved with primer pair R (Figure 2). Although the probe-binding site of QUACO135 is located outside the primer pair R-based 16S rRNA gene fragment (Loy *et al.*, 2005), the closest relative of clones R10 and R11 is the clone sequence PHOS-HE23 (accession number AF314420), which is perfectly matching probe QUACO135. In summary, the comparative sequence analysis showed the presence of a diverse *Rhodocylales* community, including members of potentially novel *Rhodocyclales* lineages for which no closely related isolates are available (Figure 2) and no specific probes were included on the RHC-PhyloChip.

Based on the microarray and sequencing data, suitable rRNA-targeted probes (Table 1) were selected or newly developed and applied for quantitative FISH analysis. Relative abundances of the different probe-defined *Rhodocyclales* groups ranged between <1% and 2.6% of the bacterial biovolume detectable with the EUB338 probe set (Table 2).

Figure 1 Presence of distinct *Rhodocyclales* groups in the Aalborg East activated sludge as interpreted from 16S rRNA gene-PCR-based RHC-PhyloChip analysis. Positive probes (with identical and hierarchical specificities) of the composite RHC-PhyloChip hybridization pattern used for interpretation of the results according to the multiple probe concept (Loy and Bodrossy, 2006) are depicted in bold.

Figure 2 Phylogenetic affiliation and function of *Rhodocyclales* in Aalborg East activated sludge. 16S rRNA gene consensus tree based on maximum-likelihood analysis (AxML) performed with a 50% conservation filter for the *Betaproteobacteria*. The tree shows the affiliation of clone sequences (boldface type) retrieved by using *Rhodocyclales* subgroup-selective primer pairs A (A clones), R (R clones), and Z (Z clones) for PCR. In addition, the incubation conditions under which the different Aalborg East sludge microorganisms were active according to isotope array and MAR-FISH analyses are shown. Abbreviations: O, oxic incubation; N, anoxic incubation with nitrate; P, propionate; B, butyrate; T, toluene. A hashmark indicates that activity was confirmed by MAR-FISH, whereas an asterisk indicates that activity was only detected by MAR-FISH. Parentheses show affiliation to the different *Rhodocyclales* lineages as outlined earlier (Loy *et al.*, 2005); dotted line indicates that a sequence cluster could not be unambiguously affiliated with the respective lineage. The bar indicates 10% estimated sequence divergence. Polytomic nodes connect branches for which a relative order could not be determined unambiguously by applying neighbor-joining, maximum-parsimony and maximum-likelihood treeing methods. Percent parsimony bootstrap values are shown by filled (⩾90%) and open (75–89%) squares. Branches without squares had bootstrap values of <75%.
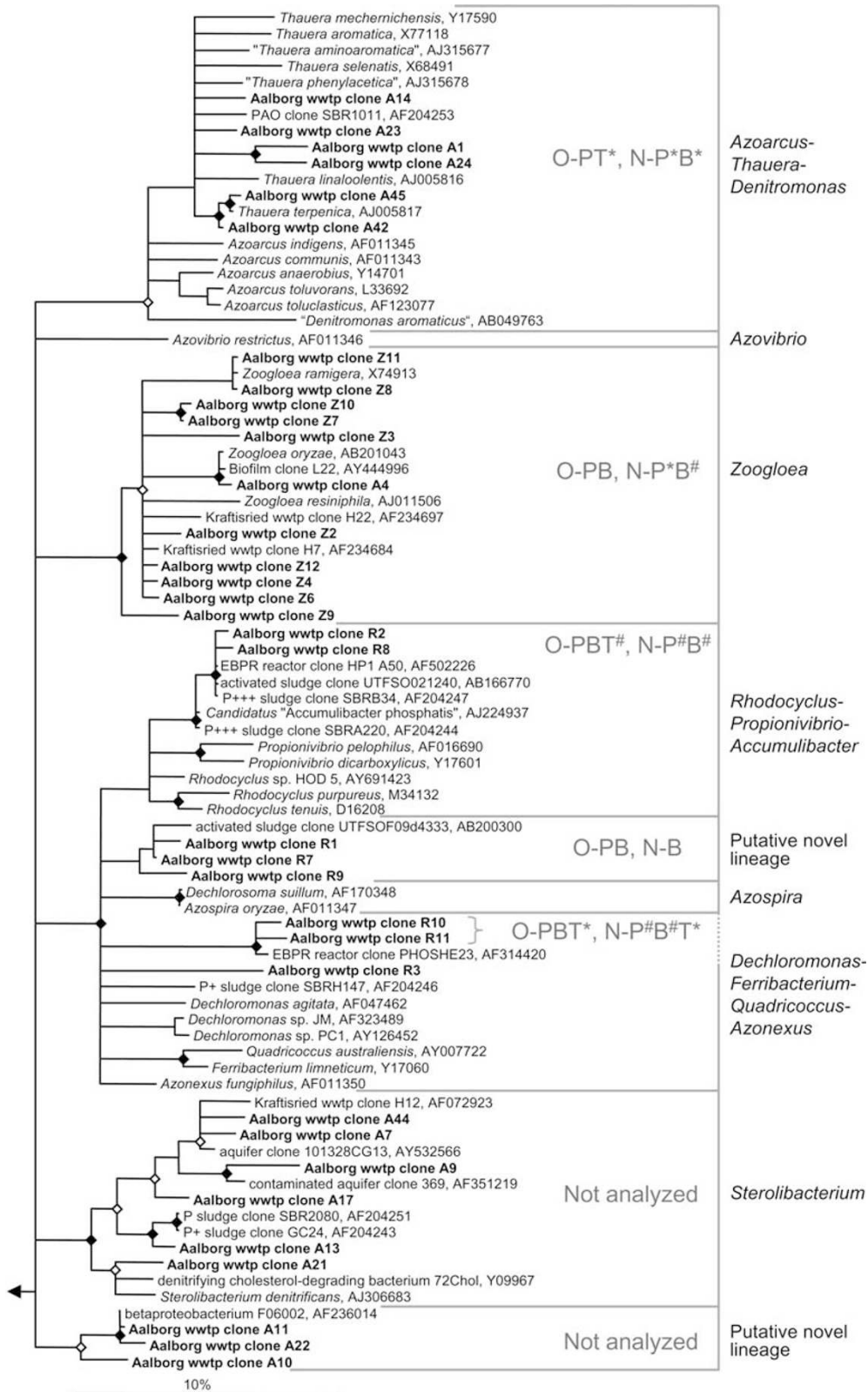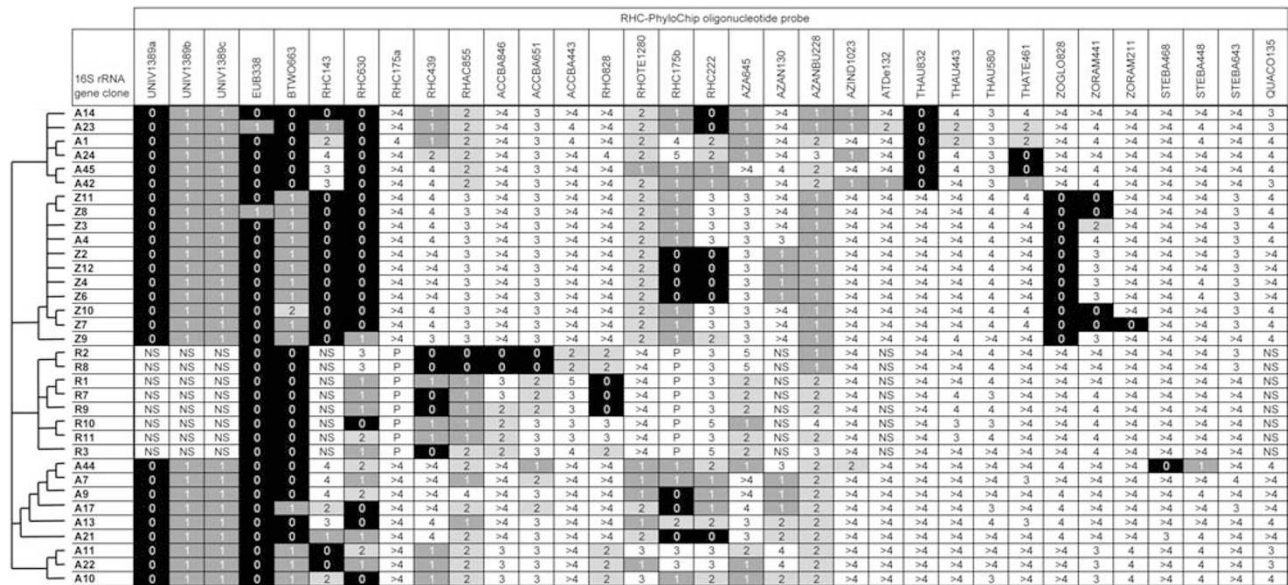
Figure 3 Number of mismatching bases in the RHC-PhyloChip probe target sites of Aalborg East clone sequences. All probes that were positive in the 16S rRNA gene PCR product-based composite RHC-PhyloChip hybridization fingerprint are shown, except of probes STEBA1426 and ZOGLO1416 that could not be analyzed because the respective target sites are only partly present on the amplified gene fragments. Clone sequences are phylogenetically ordered according to Figure 2. NS, probe-binding site is outside the amplified fragment. P, probe-binding site (partially) overlaps with the primer-binding site.

Table 2 Relative abundance and substrate uptake of different *Rhodocyclales* groups in Aalborg East activated sludge as determined by quantitative FISH and MAR-FISH, respectively

FISH probe(s) (corresponding RHC-PhyloChip probe is indicated in bold)[a]	Relative biovolume (% EUB338 probe mix)	Proportion of probe stained-cells that were MAR positive						
		Anoxic incubations with nitrate[b]					Oxic incubations[b]	
		Control (4.5 h) (%)	Propionate (4.5 h) (%)	Butyrate (4.5 h) (%)	Control (24 h) (%)	Toluene (24 h) (%)	Control (24 h) (%)	Toluene (24 h) (%)
BET42a	20.4	NA	NA	NA	NA	NA	NA	NA
AT1458 (**ATD1459**)	2.6	3	71	78	7	9	0	16
PAO651 (**ACCBA651**)	2.5	NC	NC	100	NC	NC	NC	NC
RHC439 (**RHC439**)	2.1	NC	76	30	49	84	24	30
PAO651+RHC439	1.3	4	100	100	26	36	4	32
RHC445+RHC827	1	5	18	37	3	25	3	44
ZOGLO1416 (**ZOGLO1416**)	1.1	0	55	71	NA	NA	NA	NA
ZOGLO1416+ZORAM441	<1	0[c]	50[c]	32[c]	NA	NA	NA	NA
ZOGLO1416+ZOGLO454	<1	0	7[c]	0	NA	NA	NA	NA

Abbreviations: NA, not analyzed; NC, no target cells were found in the activated sludge cross-sections that were prepared for MAR-FISH.
[a]Numbers refer to cells that gave positive signals with all listed probes.
[b]Incubation time is indicated in brackets.
[c]Value is based on <10 target cells.

Isotope labeling of RNA

The efficiency of the heterotrophic $^{14}CO_2$-assimilation labeling strategy (Hesselsoe *et al.*, 2005) was initially evaluated for labeling of RNA from propionate-utilizing organisms in Aalborg East activated sludge. Anoxic and oxic incubations with unlabeled propionate plus $^{14}CO_2$ yielded considerably higher levels of radioactivity in the extracted RNA than incubations with [^{14}C]propionate and unlabeled propionate (Table 3). Hence, $^{14}CO_2$ was used as the only isotope source for incubations of activated sludge with butyrate and toluene. In addition, control incubations without additional substrates were performed for all conditions and showed considerably less incorporation of isotope in biomass and purified RNA (Table 3).

Optimization of the RHC-PhyloChip for isotope array analysis

Earlier optimization of the RHC-PhyloChip only focused on hybridization with random-prime-labeled 16S rRNA gene PCR products (Loy *et al.*, 2005). A published protocol for hybridization of

Table 3 Labeling efficiency of biomass and RNA after incubation of activated sludge with ^{14}C-labeled substrates under different conditions

| Incubation conditions				Incubation time (h)	Labeling efficiency		
Substrate	Electron acceptor	Isotope	Radioactivity ($\mu Ci\,ml^{-1}$ activated sludge)		^{14}C in biomass (% of added radioactivity)	^{14}C in purified RNA (% of added radioactivity)	^{14}C in purified RNA ($nCi\,ml^{-1}$ activated sludge)
Propionate	Oxygen	[^{14}C]propionate	20	4.5	2.320	0.002	0.5
Propionate	Nitrate	[^{14}C]propionate	20	4.5	1.190	0.002	0.4
—	Oxygen	$^{14}CO_2$	120	4.5	0.650	0.024	28.4
—	Nitrate	$^{14}CO_2$	120	4.5	0.560	0.016	19.2
Propionate	Oxygen	$^{14}CO_2$	120	4.5	2.390	0.093	111.7
Propionate	Nitrate	$^{14}CO_2$	120	4.5	2.820	0.051	61.8
Butyrate	Oxygen	$^{14}CO_2$	120	4.5	1.600	0.105	125.5
Butyrate	Nitrate	$^{14}CO_2$	120	4.5	1.080	0.050	60.5
—	Oxygen	$^{14}CO_2$	200	24	0.350	0.005	10.3
—	Nitrate	$^{14}CO_2$	200	24	0.475	0.002	3.1
Toluene	Oxygen	$^{14}CO_2$	200	24	1.651	0.023	45.2
Toluene	Nitrate	$^{14}CO_2$	200	24	1.125	0.007	13.7

non-fragmented, native RNA (Adamczyk *et al.*, 2003) was initially adapted for use with fragmented RNA. For this purpose, separate RHC-PhyloChips were hybridized with 0.75 μg of *in vitro* transcribed, fluorescently labeled and fragmented 16S rRNA from the reference clone S3 (accession number AF072918) under different stringencies, that is, at 5%, 10%, 15%, 20%, 25% and 30% formamide in the hybridization buffer. As expected, the specificity index (the difference in mean cumulative fluorescence signal intensity between perfectly matched and mismatched probes) increased by a factor of ∼2 with increasing formamide concentration, whereas the signal intensity constantly decreased (Figure 4). To maintain a relatively high level of sensitivity (that is, high signal intensity of a probe with its perfectly matched RNA), 10% formamide in the hybridization buffer was used for all subsequent hybridizations with native RNA as a compromise between specificity (that is, the tendency of some probes to cross-react with mismatching target RNA) and sensitivity. The multiple probe concept, which formed the basis during the design of the RHC-PhyloChip (Loy *et al.*, 2005), alleviates problems that are due to unspecific hybridizations of individual probes at a lower stringency (Loy and Bodrossy, 2006).

Less than 0.1% of the added isotope was generally incorporated into community RNA during the isotopic labeling incubations (Table 3). To determine the optimal amount of ^{14}C-labeled, fragmented RNA per hybridization, separate RHC-PhyloChips were hybridized with 0.3–10 μg of Aalborg East activated sludge RNA (Figure 5). The cumulative radioactivity per probe spot on the RHC-PhyloChip increased with increasing RNA amount and no signal saturation was observed within the RNA concentration range tested. In contrast, use of higher RNA amounts improves the detection limit of the isotope array

approach. In contrast, hybridization under probe-saturated, target-excess conditions (that is, conditions under which most of the probe molecules on a spot have bound a target molecule) impairs reliable quantification of probe signals (Schena, 2003). Six (from the propionate, butyrate, and the corresponding control incubations) or 10 μg of RNA (from the toluene and the corresponding control incubations) were thus used for each further isotope array hybridization.

Isotope array analysis of Rhodocyclales *in activated sludge*
A separate RHC-PhyloChip was hybridized with fluorescently labeled and fragmented RNA from each activated sludge subsample that was incubated with $^{14}CO_2$ and allylthiourea under different conditions (Table 3). An activity and substrate-utilization profile of the different *Rhodocyclales* groups in the activated sludge was created (Table 4) based on the presence–absence of radioactive probe signals after isotope array analysis (Supplementary online Tables) and the retrieved 16S rRNA gene sequences (Figures 2 and 3). Radioactive signals of microarray probe QUACO135 in all hybridizations indicated that bacteria represented by clones R10 and R11 were active under all conditions tested. In contrast, the isotope array analyses further suggested that all other *Rhodocyclales* groups, for which specific probes were present on the RHC-PhyloChip, displayed more specialized substrate-incorporation behaviors. For example, radioactive 16S rRNA from members of the genus *Zoogloea* and from a putative novel *Rhodocyclales* lineage (represented by clones R1, R7 and R9) was detectable after oxic incubation with butyrate and propionate, but not with toluene. Under nitrate-reducing conditions, only hybridization of RNA that was extracted from the incubation
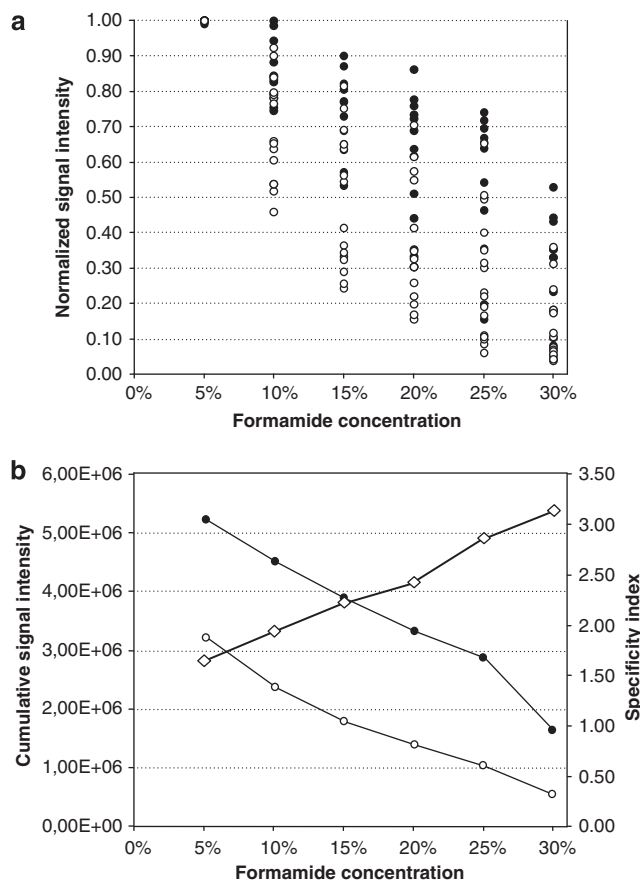
Figure 4 Signal intensities of probes forming detectable, perfectly matched and mismatched hybrids with fragmented, fluorescently labeled 16S rRNA from reference clone S3 (AF072918) at different formamide concentrations in the hybridization buffer. (**a**) normalized signal intensities of three replicate spots are shown for each perfectly matching probe (closed circles) and each probe with one, two or three mismatch(es) (open circles). Cumulative fluorescence intensity of each probe was normalized with the highest intensity of this probe observed at the different stringencies. (**b**) (left *Y*-axis); mean cumulative signal intensity of all perfectly matched probes (closed circles) and of all probes with one to three mismatches (open circles) are indicated. (right *Y*-axis); open diamonds indicate the specificity index at a given stringency, that is, the ratio of the mean signal intensity of all perfectly matched probes versus the mean signal intensity of all probes with one to three mismatches, for each formamide concentration.

with butyrate yielded radioactive signals with a genus *Zoogloea*-specific probe and the probe RHO828, fully matching clones R1, R7 and R9 (Figures 2 and 3).

By assuming an unbiased fluorescence-labeling step and that each probe hybridized only to its perfectly matched target organisms, the *A*-values were used to infer changes in heterotrophic $^{14}CO_2$-assimilation activity of probe-defined populations. Addition of electron donors stimulated incorporation of ^{14}C into rRNA in all experiments, that is, yielded higher *A*-values in comparison with the control samples (Figure 6). For example, addition of each of the three substrates under oxic conditions caused a five- to sixfold increase in the *A*-value

for probe QUACO135. An even higher increase was observed for probe QUACO135 under denitrifying conditions in the presence of propionate and butyrate, but toluene seemed to stimulate heterotrophic $^{14}CO_2$ assimilation only moderately (Figure 6).

### MAR-FISH analysis of Rhodocyclales *in activated sludge*

For independent confirmation of the isotope array results, substrate incorporation was also analyzed at the single-cell level for selected incubations and *Rhodocyclales* groups by MAR-FISH (Table 2). MAR-FISH results obtained with probes AT1458, PAO651, RHC439 and ZOGLO1416 could be directly compared with isotope array results because corresponding probes were present on the RHC-PhyloChip. With one exception, similar results were obtained with both techniques. Although MAR-FISH with probe ZOGLO1416 clearly showed that $^{14}CO_2$ assimilation of *Zoogloea* species was enhanced during anoxic incubation with propionate and nitrate, no radioactivity was recorded on the isotope array with the same probe. This suggests that the amount and specific radioactivity of *Zoogloea* 16S rRNA was below the detection limit of probe ZOGLO1416, when it was applied in the microarray format. In addition, newly developed probes with a narrower target range for the Aalborg East activated sludge clones were used for MAR-FISH analysis at a higher phylogenetic resolution than offered by the current RHC-PhyloChip probe set. Application of probes ZOGLO441 and ZOGLO454, differentiating between two *Zoogloea* clone groups in the activated sludge, indicated that both the probe-defined populations reduced nitrate anaerobically with propionate. In contrast, only ZOGLO441-targeted cells were MAR positive in anoxic incubations with nitrate and butyrate.

The MAR-positive signals were also observed for cells detected by the new RHC445–RHC827 probe combination (targeting clones R10 and R11 that are presumably also targeted by RHC-PhyloChip probe QUACO135) in all samples analyzed (Table 2). Compared with the control, considerably larger proportions of MAR-positive cells were observed in incubations with substrates, clearly indicating that the RHC445–RHC827 probe-defined population metabolized the offered substrates.

Discussion

Methodological and conceptual considerations for isotope array analysis

Additional modifications of the original isotope array protocol (Adamczyk *et al.*, 2003) were introduced in this study and their implications for inferring biologically meaningful data are highlighted in the following section. General strengths
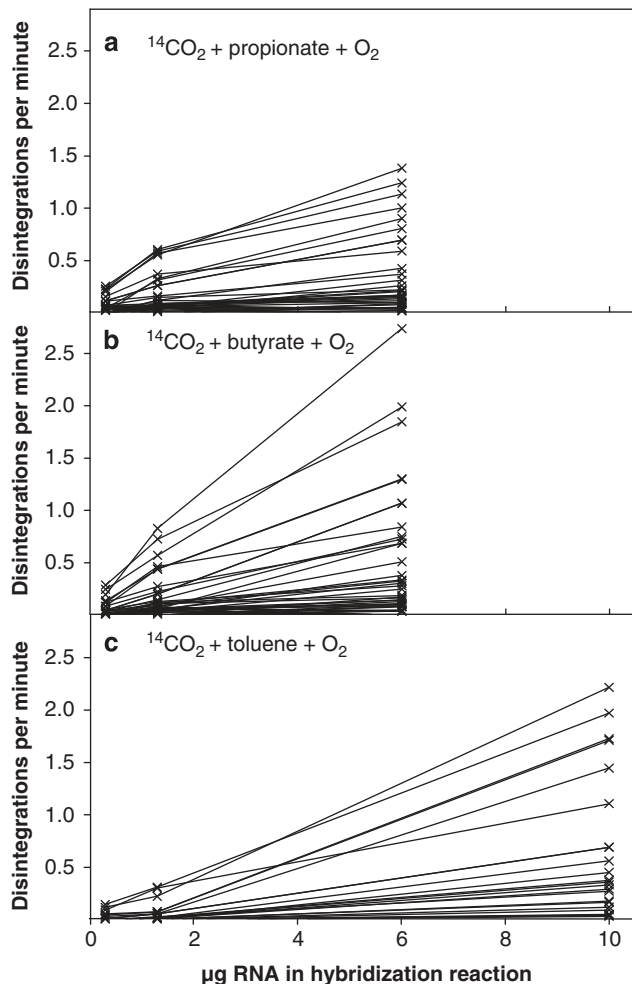
Figure 5 Mean radioactivity of RHC-PhyloChip probes after hybridization with different amounts of ^{14}C-labeled RNA. Fragmented, community RNA was prepared from oxic incubations of activated sludge with $^{14}CO_2$ and (**a**) propionate, (**b**) butyrate or (**c**) toluene.

and limitations of the isotope array approach have been discussed earlier and are thus not explicitly mentioned (Adamczyk *et al.*, 2003; Wagner *et al.*, 2006; Neufeld *et al.*, 2007).

Metabolically active heterotrophic microorganisms assimilate CO_2 through various carboxylation reactions (Roslev *et al.*, 2004) catalyzed by enzymes, such as pyruvate carboxylase, phosphoenolpyruvate carboxylase and coenzyme A carboxylase (Barker, 1941; Dijkhuizen and Harder, 1985). In analogy to the HetCO$_2$-MAR variant of MAR-FISH (Hesselsoe *et al.*, 2005), the CO$_2$-assimilating ability of heterotrophic microorganisms was employed for radioactive labeling of community members metabolizing a substrate in the presence of radioactive $^{14}CO_2$. In this approach, consumption of non-radioactive substrates is measured indirectly through $^{14}CO_2$ incorporation. It is therefore necessary to perform $^{14}CO_2$ control experiments without the addition of organic substrates. Subsequent differential display

analysis of the isotope array data of the control and the actual experiment distinguishes between background CO_2 assimilation (for example, driven by metabolization of cellular storage compounds) and CO_2 assimilation that is additionally induced by the added substrate. Furthermore, the relative, substrate-induced increase in CO_2-assimilating activity of a probe-defined population can be assessed through the *A*-value (Figure 6). Although additional control experiments must be performed, this indirect $^{14}CO_2$-based labeling strategy has several advantages over the alternative isotope-labeling approach for analyzing the metabolization of an organic substrate, that is, the incubation of a sample with the radioactive organic substrate, but without $^{14}CO_2$ (Hesselsoe *et al.*, 2005). First, $^{14}CO_2$ is available with maximal specific radioactivity ($>99\%$ of C atoms are ^{14}C) and is relatively inexpensive. Therefore, it can be applied economically in high quantities. Second, the variety of commercially available ^{14}C-labeled organic substrates, especially of large molecules, is limited and their specific radioactivity ($\%^{14}C$ content) is often low. Homogeneously isotope-labeled complex substrates are often not commercially available at all or very expensive. In our test experiments, community RNA was significantly more strongly labeled after incubation with $^{14}CO_2$ and unlabeled propionate than after incubation with [^{14}C]propionate and unlabeled propionate (Table 3). However, the labeling efficiency of the latter incubation might be improved by adjusting the ratio between the concentrations of radioactive and non-radioactive substrate (1:11.8 for unlabeled/^{14}C-labeled propionate in this study) and the $\%^{14}C$ content of the added substrate ($\sim 33\%$ of C atoms were ^{14}C in the [^{14}C]propionate used in this study). We suggest that the heterotrophic CO$_2$-assimilation labeling strategy offers additional flexibility in the design of isotope array experiments and, at least in cases where large organic molecules are only available with one or a few ^{14}C atoms, also might improve the detection limit of the isotope array.

The sensitivity of the isotope array generally depends on the abundance (that is, absolute and relative rRNA content) and on the specific substrate-assimilation rate (that is, the rate at which substrate-derived ^{14}C is incorporated into *in vivo* synthesized rRNA) of a probe-defined target population (Adamczyk *et al.*, 2003). The detection limit for different probe-defined populations at a given hybridization condition will further vary owing to the different thermodynamic properties of the probes. For instance, members of the genus *Zoogloea*, comprising only about 1% of the bacterial biovolume in the Aalborg East activated sludge, are targeted by the genus-specific microarray probes ZOGLO828 and ZOGLO1416 with a theoretical free binding energy (ΔG_{12}) of -17.94 and $-20.27\,kcal\,mol^{-1}$, respectively. The difference in free binding energy could

Table 4 Phylogenetic and functional profile of *Rhodocyclales* in the Aalborg East activated sludge as inferred from presence/absence of radioactive probe signals after RHC-Isotope Array and 16S rRNA gene clone library analyses

Activated sludge clone sequences	Phylogenetic affiliation	Nested probe set perfectly-matching the respective activated sludge clones	Oxic incubation				Anoxic incubation with nitrate			
			Control (no electron donor added)	Propionate	Butyrate	Toluene	Control (no electron donor added)	Propionate	Butyrate	Toluene
Z2, Z3, Z4, Z6, Z7, Z8, Z9, Z10, Z11, Z12, A4	Genus *Zoogloea*	UNIV1389a, EUB338, RHC143, RHC630, ZOGLO1416, ZOGLO828	–	+	+	–	–	–	(+)[a]	–
A1, A14, A23, A24[b], A42, A45[b]	Genus *Thauera*	UNIV1389a, EUB338, BTWO663, RHC630, ATD1459[g], THAU832	–	+	–	–	–	–	–	–
R2, R8	Genus '*Candidatus* Accumulibacter'	UNIV1389a, EUB338, BTWO663, RHC439, RHAC855, ACCBA846, ACCBA651	(+)[c]	+	+	(+)[c]	–	(+)[c]	(+)[c]	–
R1[d], R7, R9	Putative novel *Rhodocyclales* lineage	UNIV1389a, EUB338, BTWO663, RHC439, RHO828	–	+	+	–	–	–	+	–
R10, R11[e]	*Dechloromonas–Ferribacterium–Quadricoccus–Azonexus* lineage	UNIV1389a, EUB338, BTWO663, QUACO135[d]	+	+	+	+	+	+	+	+
A7, A9, A13, A17, A21, A44[f]	*Sterolibacterium* lineage	UNIV1389a, EUB338, BTWO663	NA	NA	NA	NA	NA	NA	NA	NA
A10, A11, A22	Putative novel *Rhodocyclales* lineage	UNIV1389a, EUB338	NA	NA	NA	NA	NA	NA	NA	NA

+, All probes in the nested probe set showed a radioactive signal; −, probes with the narrowest target specificity in the nested probe set showed no radioactive signal. NA, probes targeting the clone sequences at higher specificity were not present on the RHC-PhyloChip and thus substrate utilization could not be analyzed for these phylogenetic groups.
[a]Probe ZOGLO828 showed no radioactive signal.
[b]A24 and A45 perfectly match probe THATE461, which showed no radioactive signal in all experiments.
[c]Probe ACCBA846 showed no radioactive signal.
[d]R1 contains a weak mismatch (0.6 weighted mismatch) to probe RHC439.
[e]The amplified sequence fragments of clones R10 and R11 do not include the probe QUACO135 target region, but the clones are most closely related to sequence PHOS-HE23, AF314420, which perfectly matches QUACO135.
[f]A44 perfectly match probe STEBA468, which showed no radioactive signal in all experiments.
[g]Binding site for probe ATD1459 is outside the amplified and sequenced 16S rRNA gene fragment.

explain why only probe ZOGLO1416 showed radioactivity after isotope array analysis of the sample exposed to butyrate under denitrifying conditions (Figure 6 and Table 4). However, the efficiency of a microarray probe to hybridize with its target (N.B.: the signal intensity of the resulting probe-target hybrid is often used as proxy for this efficiency) is strongly dependent on the experimental conditions, such as target preparation and hybridization procedures, factors which are currently not adequately addressed by available algorithms for calculating the free energy of a probe-target hybridization event. Theoretical ΔG values will thus inevitably not always correlate with the actual probe signal intensities (Pozhitkov *et al.*, 2006). Hence, an alternative explanation for the observed discrepancy in signal intensities for probes ZOGLO828 and ZOGLO1416 is that they differ in their coverage of target organisms and/or tendency to cross-hybridize with non-target organisms.

For hybridization signals above the detection threshold, the *A*-value could theoretically compensate for the different binding efficiencies of different probes. However, quantification using the *A*-value is susceptible to systematic biases. The direct fluorescence labeling of RNA method used in this study attaches Cy-dye molecules covalently to guanine residues. Thus, organisms with a guanine-rich 16S rRNA could contain more dye molecules per RNA molecule, underestimating their *A*-value-based substrate-utilization rate compared with guanine-poorer organisms. It is noteworthy that this bias is less profound for microarray probes targeting a phylogenetically narrow range of microorganisms with no or little variation in their 16S rRNA guanine contents. Accuracy of the *A*-value further depends on the specificity of the respective microarray probe. Although these sources of errors generally hamper comparisons among different probe-defined populations, the *A*-value still offers the possibility to monitor relative changes in substrate incorporation activity of a given probe-defined population under different environmental conditions.
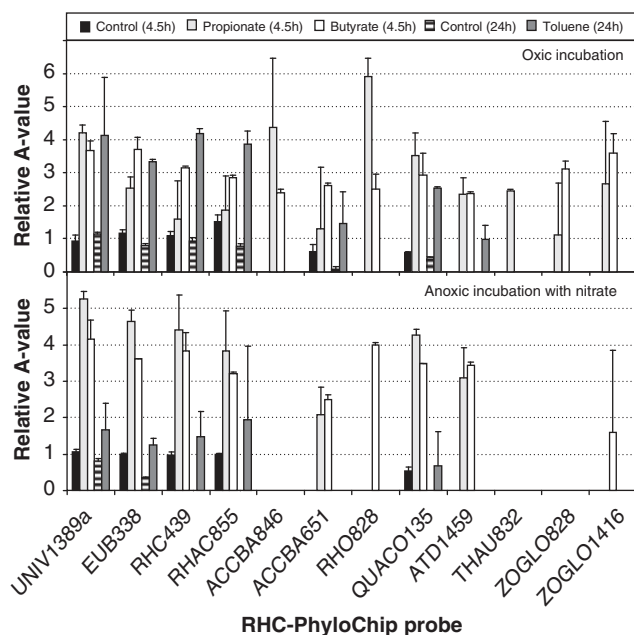
Figure 6 Relative *A*-values of selected RHC-PhyloChip probes after isotope array analysis of activated sludge. The *A*-value of each probe was divided by the mean *A*-value of the universal probes (UNIV1389a, UNIV1389b and UNIV1389c) recorded on reference slides that were hybridized with a corresponding control sample (that is, a sample that was incubated with $^{14}CO_2$ under the same conditions without addition of electron donor).

In summary, the described modifications of the isotope array protocol, including the adaptation of a heterotrophic $^{14}CO_2$-assimilation-based isotope labeling, improved the sensitivity of the technique and enabled detection of native, radioactive 16S rRNA extracted from low-abundant (relative abundance of ~1% of the total bacterial biovolume as analyzed by quantitative FISH), but active members of a complex-activated sludge community.

Diversity and ecophysiology of Rhodocyclales *in Aalborg East activated sludge*
In this study, we showed the diversity and some potential nutritional niches of bacteria belonging to the order *Rhodocyclales* in a nitrogen- and phosphorus-removing, full-scale wastewater treatment plant. Identification and quantification of members of the *Rhodocyclales* followed the same RHC-PhyloChip-centric strategy as outlined in an earlier study (Loy *et al.*, 2005). For functional analysis of *Rhodocyclales* using the isotope array approach, the RHC-PhyloChip was newly adapted for hybridization of native community rRNA.

The Aalborg East activated sludge contained an estimated number of 27 different *Rhodocyclales* OTUs, which belonged to at least seven different lineages (Figure 2). The presence of a high *Rhodocyclales* richness in denitrifying wastewater treatment systems is consistent with earlier observations

(Juretschko *et al.*, 2002; Ginige *et al.*, 2005; Liu *et al.*, 2006; Thomsen *et al.*, 2007; Morgan-Sagastume *et al.*, 2008). In contrast to these studies, the relative abundance of selected *Rhodocyclales* groups did not exceed 2.6% of the total bacterial biovolume (Table 2). However, combined interpretation of isotope array and MAR-FISH data showed that all *Rhodocyclales* groups, for which specific probes were applied, were active and metabolized (some of) the offered electron donors in the presence of oxygen and/or under anoxic nitrate-reducing conditions (Figures 2 and 6, Tables 2 and 4). Aside from the involvement in nitrogen transformation, one can further speculate about the ecophysiology of the different *Rhodocyclales* groups on the basis of their activity pattern recorded for the different incubation conditions.

'*Candidatus* Accumulibacter' species and members of the *Dechloromonas–Ferribacterium–Quadricoccus–Azonexus*-related group (represented by clones R10 and R11) were the only metabolically active groups in the control incubations, under substrate depletion (Table 4). Background $^{14}CO_2$ assimilation by these organisms could result from mobilization of intracellular compounds that are stored for bridging the unavoidable phases of nutrient limitation (Hesselsoe *et al.*, 2005). The capacity for anaerobically storing poly-β-hydroxy alkanoates puts polyphosphate-accumulating '*Candidatus* Accumulibacter' species in a selective advantage during enhanced biological phosphorus removal (Blackall *et al.*, 2002). Therefore, one might argue that bacteria represented by clones R10 and R11 are also linked to this process. Whether these bacteria truly have the beneficial polyphosphate-accumulating phenotype or are glycogen non-polyphosphate-accumulating organisms, which also synthesize poly-β-hydroxy alkanoates anaerobically but are detrimental for the enhanced biological phosphorus removal process, remains to be elucidated (Kong *et al.*, 2004, 2006). The FISH probe set RHC445–RHC827, developed in this study (Table 1), is a molecular tool for proving this hypothesis in future MAR-FISH experiments.

Our results further support earlier findings that some polyphosphate-accumulating organisms are also capable of reducing nitrate in wastewater treatment systems (Zeng *et al.*, 2003; Kong *et al.*, 2004; Thomsen *et al.*, 2007; Morgan-Sagastume *et al.*, 2008). Both, the '*Candidatus* Accumulibacter' species and the bacteria of the *Dechloromonas–Ferribacterium–Quadricoccus–Azonexus*-related group, showed moderately to strongly enhanced biosynthesis when they were exposed to propionate, butyrate or toluene under nitrate-reducing conditions (Figure 6, Table 2). It remains to be shown whether these organisms are truly denitrifiers or only catalyze the reduction of nitrate to nitrite.

Aromatic hydrocarbons, such as toluene, can occasionally occur in municipal wastewater through contamination with oil, gasoline and industrial waste (Eriksson *et al.*, 2003; Dincer and Muezzino-

glu, 2008). Toluene was selected as one of the substrates analyzed in this study because (i) the capability for aerobic and anaerobic aromatic compound degradation is widespread among strains from different *Rhodocyclales* lineages, such as *Thauera* sp. DNT-1 (Shinoda *et al.*, 2004) or *Dechloromonas* sp. RCB (Chakraborty *et al.*, 2005) and (ii) pre-experiments have shown that the Aalborg East activated sludge has the capacity for anaerobic and aerobic toluene degradations (data not shown). Apart from being involved in nitrogen- and phosphorus removal, we hypothesized that wastewater *Rhodocyclales* are also responsible for biodegradation of aromatic hydrocarbons in wastewater. Consistently, several probe-defined populations showed increased $^{14}CO_2$ assimilation activity on exposure to toluene in the isotope array and MAR-FISH experiments (Figure 6, Table 2). This finding clearly highlights the aromatic compound decontamination potential offered by the *Rhodocyclales* communities in wastewater treatment plants.

It is likely that microorganisms for which no specific probes were applied, such as members of the *Sterolibacterium* lineage (Tarlera and Denner, 2003) and the putative novel *Rhodocyclales* lineage (represented by clones A10, A11 and A22) (Figure 2), and other microorganisms (Morgan-Sagastume *et al.*, 2008), also contributed to anaerobic nitrate reduction in this wastewater treatment plant. Nevertheless, our data show that a high functional redundancy, regarding the ability for anaerobic nitrate reduction (and thus potentially for denitrification), existed within the diverse *Rhodocyclales* community in the activated sludge (Table 4, Figures 2 and 6). Substrate-utilization profiles of the different *Rhodocyclales* groups further indicate that they (i) occupied partially overlapping nutritional niches in the wastewater ecosystem and (ii) might differ in their adaptation to fluctuations in the organic compound composition of wastewater. A rather generalist substrate-consumption behavior was exhibited by 'Candidatus Accumulibacter' species and members of the *Dechloromonas–Ferribacterium–Quadricoccus–Azonexus*-related group (represented by clones R10 and R11), whereas other *Rhodocyclales* groups such as *Thauera* and *Zoogloea* seemed to be more specialized. It is self-evident that the implementation of additional substrates, incubation conditions and parameters such as substrate affinities and incorporation rates in the isotope array testing regime would show even more detailed information on the extent of niche overlap and substrate specialization of *Rhodocyclales* in this activated sludge.

In conclusion, by application of the isotope array in concert with other complementary techniques, we showed the functional versatility and redundancy of a diverse *Rhodocyclales* community in activated sludge from a full-scale wastewater treatment plant, lending further weight to the importance of members of this taxon for removal of

environmental pollutants. We further anticipate that the future of the isotope array techniques lies within its adaptation for the analysis of stable isotopes by using Raman microspectroscopy or nanoSIMS. Technical limitations of these instruments, such as the long image acquisition time of the nanoSIMS for analyzing large areas of interest (Musat *et al.*, 2008), currently still hinder their application for microarray analysis. However, the high spatial resolution of both techniques would theoretically allow exploiting high-density microarrays consisting of thousands of small probe spots ($<50 \mu m$ in diameter). This option is currently not available for the radioactive isotope array approach because of the low spatial resolution of β-imagers. The high sensitivity of the nanoSIMS (Wagner, 2009) even gives hope for simultaneous analysis of gene expression and substrate utilization by functional gene array-based detection (He *et al.*, 2007) of stable isotope-labeled mRNA. Highly parallel analysis of physiological properties of many phylogenetically different community members is a looked-for option in microbial ecology. The isotope array method thus has much promise to unfolding the complex nutritional networks of uncultivated microorganisms living in multiorganism assemblages.

Acknowledgements

References

Aakra A, Hesselsoe M, Bakken LR. (2000). Surface attachment of ammonia-oxidizing bacteria in soil. *Microb Ecol* **39**: 222–235.

Adamczyk J, Hesselsoe M, Iversen N, Horn M, Lehner A, Nielsen PH *et al.* (2003). The isotope array, a new tool that employs substrate-mediated labeling of rRNA for determination of microbial community structure and function. *Appl Environ Microbiol* **69**: 6875–6887.

Alm EW, Oerther DB, Larsen N, Stahl DA, Raskin L. (1996). The oligonucleotide probe database. *Appl Environ Microbiol* **62**: 3557–3559.

Amann RI, Krumholz L, Stahl DA. (1990). Fluorescent-oligonucleotide probing of whole cells for determinative, phylogenetic, and environmental studies in microbiology. *J Bacteriol* **172**: 762–770.

Barker HA. (1941). The chemistry and metabolism of bacteria. *Annu Rev Biochem* **10**: 553–580.

Bedard C, Knowles R. (1989). Physiology, biochemistry, and specific inhibitors of CH_4, NH_4^+, and CO oxidation

by methanotrophs and nitrifiers. *Microbiol Rev* **53**: 68–84.

Behrens S, Losekann T, Pett-Ridge J, Weber PK, Ng WO, Stevenson BS *et al.* (2008). Linking microbial phylogeny to metabolic activity at the single-cell level by using enhanced element labeling-catalyzed reporter deposition fluorescence *in situ* hybridization (EL-FISH) and nanoSIMS. *Appl Environ Microbiol* **74**: 3143–3150.

Blackall LL, Crocetti GR, Saunders AM, Bond PL. (2002). A review and update of the microbiology of enhanced biological phosphorus removal in wastewater treatment plants. *Antonie Van Leeuwenhoek* **81**: 681–691.

Bodrossy L, Sessitsch A. (2004). Oligonucleotide microarrays in microbial diagnostics. *Curr Opin Microbiol* **7**: 245–254.

Chai XS, Lou Q, Zhu JY. (2001). Analysis of nonvolatile species in a complex matrix by headspace gas chromatography. *J Chromatogr A* **909**: 249–257.

Chakraborty R, O'Connor SM, Chan E, Coates JD. (2005). Anaerobic degradation of benzene, toluene, ethylbenzene, and xylene compounds by *Dechloromonas* strain RCB. *Appl Environ Microbiol* **71**: 8649–8655.

Cole JR, Chai B, Farris RJ, Wang Q, Kulam SA, McGarrell DM *et al.* (2005). The Ribosomal Database Project (RDP-II): sequences and tools for high-throughput rRNA analysis. *Nucleic Acids Res* **33**: 294–296.

Crocetti GR, Hugenholtz P, Bond PL, Schuler A, Keller J, Jenkins D *et al.* (2000). Identification of polyphosphate-accumulating organisms and design of 16S rRNA-directed probes for their detection and quantitation. *Appl Environ Microbiol* **66**: 1175–1182.

Daims H, Brühl A, Amann R, Schleifer K-H, Wagner M. (1999). The domain-specific probe EUB338 is insufficient for the detection of all *bacteria*: development and evaluation of a more comprehensive probe set. *Syst Appl Microbiol* **22**: 434–444.

Daims H, Lücker S, Wagner M. (2006). daime, a novel image analysis program for microbial ecology and biofilm research. *Environ Microbiol* **8**: 200–213.

Daims H, Stoecker K, Wagner M. (2005). Fluorescence *in situ* hybridization for the detection of prokaryotes. In: Osborn AM, Smith CJ (eds). *Advanced Methods in Molecular Microbial Ecology*. BIOS Scientific Publishers: Abingdon, UK. pp 213–239.

Dijkhuizen L, Harder W. (1985). Microbial metabolism of carbon dioxide. In: H Dalton (ed). *Comprehensive Biotechnology, the Principles of Biotechnology*. Pergamon Press, Ltd.: Oxford, England. pp 409–423.

Dincer F, Muezzinoglu A. (2008). Odor-causing volatile organic compounds in wastewater treatment plant units and sludge management areas. *J Environ Sci Health A Tox Hazard Subst Environ Eng* **43**: 1569–1574.

Eriksson E, Auffarth K, Eilersen A-M, Henze M, Ledin A. (2003). Household chemicals and personal care products as sources for xenobiotic organic compounds in grey wastewater. *Water SA* **29**: 135–146.

Etchebehere C, Cabezas A, Dabert P, Muxi L. (2003). Evolution of the bacterial community during granules formation in denitrifying reactors followed by molecular, culture-independent techniques. *Water Sci Technol* **48**: 75–79.

Friedrich MW. (2006). Stable-isotope probing of DNA: insights into the function of uncultivated microorganisms from isotopically labeled metagenomes. *Curr Opin Biotechnol* **17**: 59–66.

Ginige MP, Keller J, Blackall LL. (2005). Investigation of an acetate-fed denitrifying microbial community by stable isotope probing, full-cycle rRNA analysis, and fluorescent *in situ* hybridization-microautoradiography. *Appl Environ Microbiol* **71**: 8683–8691.

He Z, Gentry TJ, Schadt CW, Wu L, Liebich J, Chong SC *et al.* (2007). GeoChip: a comprehensive microarray for investigating biogeochemical, ecological and environmental processes. *ISME J* **1**: 67–77.

Hesselmann RPX, Werlen C, Hahn D, van der Meer JR, Zehnder AJB. (1999). Enrichment, phylogenetic analysis and detection of a bacterium that performs enhanced biological phosphate removal in activated sludge. *Syst Appl Microbiol* **22**: 454–465.

Hesselsoe M, Nielsen JL, Roslev P, Nielsen PH. (2005). Isotope labeling and microautoradiography of active heterotrophic bacteria on the basis of assimilation of $^{14}CO_2$. *Appl Environ Microbiol* **71**: 646–655.

Huang WE, Stoecker K, Griffiths R, Newbold L, Daims H, Whiteley AS *et al.* (2007). Raman-FISH: combining stable-isotope Raman spectroscopy and fluorescence *in situ* hybridization for the single cell analysis of identity and function. *Environ Microbiol* **9**: 1878–1889.

Juretschko S, Loy A, Lehner A, Wagner M. (2002). The microbial community composition of a nitrifying-denitrifying activated sludge from an industrial sewage treatment plant analyzed by the full-cycle rRNA approach. *Syst Appl Microbiol* **25**: 84–99.

Kong Y, Nielsen JL, Nielsen PH. (2004). Microautoradiographic study of *Rhodocyclus*-related polyphosphate-accumulating bacteria in full-scale enhanced biological phosphorus removal plants. *Appl Environ Microbiol* **70**: 5383–5390.

Kong Y, Xia Y, Nielsen JL, Nielsen PH. (2006). Ecophysiology of a group of uncultured Gammaproteobacterial glycogen-accumulating organisms in full-scale enhanced biological phosphorus removal wastewater treatment plants. *Environ Microbiol* **8**: 479–489.

Lee N, Nielsen PH, Andreasen KH, Juretschko S, Nielsen JL, Schleifer K-H *et al.* (1999). Combination of fluorescent *in situ* hybridization and microautoradiography—a new tool for structure-function analyses in microbial ecology. *Appl Environ Microbiol* **65**: 1289–1297.

Lehner A, Loy A, Behr T, Gaenge H, Ludwig W, Wagner M *et al.* (2005). Oligonucleotide microarray for identification of *Enterococcus* species. *FEMS Microbiol Lett* **246**: 133–142.

Li T, Wu TD, Mazeas L, Toffin L, Guerquin-Kern JL, Leblon G *et al.* (2008). Simultaneous analysis of microbial identity and function using nanoSIMS. *Environ Microbiol* **10**: 580–588.

Liu B, Zhang F, Feng X, Liu Y, Yan X, Zhang X *et al.* (2006). *Thauera* and *Azoarcus* as functionally important genera in a denitrifying quinoline-removal bioreactor as revealed by microbial community structure comparison. *FEMS Microbiol Ecol* **55**: 274–286.

Liu WT, Mirzabekov AD, Stahl DA. (2001). Optimization of an oligonucleotide microchip for microbial identification studies: a non-equilibrium dissociation approach. *Environ Microbiol* **3**: 619–629.

Loy A, Arnold R, Tischler P, Rattei T, Wagner M, Horn M. (2008). probeCheck—a central resource for evaluating oligonucleotide probe coverage and specificity. *Environ Microbiol* **10**: 2894–2896.

Loy A, Bodrossy L. (2006). Highly parallel microbial diagnostics using oligonucleotide microarrays. *Clin Chim Acta* **363**: 106–119.

Loy A, Lehner A, Lee N, Adamczyk J, Meier H, Ernst J *et al.* (2002). Oligonucleotide microarray for 16S rRNA gene-based detection of all recognized lineages of sulfate-reducing prokaryotes in the environment. *Appl Environ Microbiol* **68**: 5064–5081.

Loy A, Maixner F, Wagner M, Horn M. (2007). probeBase—an online resource for rRNA-targeted oligonucleotide probes: new features 2007. *Nucleic Acids Res* **35**: D800–D804.

Loy A, Schulz C, Lücker S, Schöpfer-Wendels A, Stoecker K, Baranyi C *et al.* (2005). 16S rRNA gene-based oligonucleotide microarray for environmental monitoring of the betaproteobacterial order 'Rhodocyclales'. *Appl Environ Microbiol* **71**: 1373–1386.

Ludwig W, Strunk O, Westram R, Richter L, Meier H, Yadhukumar *et al.* (2004). ARB: a software environment for sequence data. *Nucleic Acids Res* **32**: 1363–1371.

Madsen EL. (2006). The use of stable isotope probing techniques in bioreactor and field studies on bioremediation. *Curr Opin Biotechnol* **17**: 92–97.

Manefield M, Whiteley AS, Griffiths RI, Bailey MJ. (2002). RNA stable isotope probing, a novel means of linking microbial community function to phylogeny. *Appl Environ Microbiol* **68**: 5367–5373.

Manz W, Amann R, Ludwig W, Wagner M, Schleifer K-H. (1992). Phylogenetic oligodeoxynucleotide probes for the major subclasses of *Proteobacteria*: problems and solutions. *System Appl Microbiol* **15**: 593–600.

Morgan-Sagastume F, Nielsen JL, Nielsen PH. (2008). Substrate-dependent denitrification of abundant probe-defined denitrifying bacteria in activated sludge. *FEMS Microbiol Ecol* **66**: 447–461.

Musat N, Halm H, Winterholler B, Hoppe P, Peduzzi S, Hillion F *et al.* (2008). A single-cell view on the ecophysiology of anaerobic phototrophic bacteria. *Proc Natl Acad Sci USA* **105**: 17861–17866.

Neufeld JD, Wagner M, Murrell JC. (2007). Who eats what, where and when? Isotope-labelling experiments are coming of age. *ISME J* **1**: 103–110.

Ouverney CC, Fuhrman JA. (1999). Combined microautoradiography-16S rRNA probe technique for determination of radioisotope uptake by specific microbial cell types *in situ*. *Appl Environ Microbiol* **65**: 1746–1752.

Palmer C, Bik EM, Eisen MB, Eckburg PB, Sana TR, Wolber PK *et al.* (2006). Rapid quantitative profiling of complex microbial populations. *Nucleic Acids Res* **34**: e5.

Pozhitkov A, Noble PA, Domazet-Loso T, Nolte AW, Sonnenberg R, Staehler P *et al.* (2006). Tests of rRNA hybridization to microarrays suggest that hybridization characteristics of oligonucleotide probes for species discrimination cannot be predicted. *Nucleic Acids Res* **34**: e66.

Rabus R, Wilkes H, Schramm A, Harms G, Behrends A, Amann R *et al.* (1999). Anaerobic utilization of alkylbenzenes and n-alkanes from crude oil in an enrichment culture of denitrifying bacteria affiliating with the beta-subclass of *Proteobacteria*. *Environ Microbiol* **1**: 145–157.

Radajewski S, Ineson P, Parekh NR, Murrell JC. (2000). Stable-isotope probing as a tool in microbial ecology. *Nature* **403**: 646–649.

Roslev P, Larsen MB, Jorgensen D, Hesselsoe M. (2004). Use of heterotrophic CO_2 assimilation as a measure of metabolic activity in planktonic and sessile bacteria. *J Microbiol Methods* **59**: 381–393.

Sambrook J, Russell DW. (2001). *Molecular Cloning: A Laboratory Manual*, 3rd edn. Cold Spring Harbor Laboratory Press: Cold Spring Harbor, NY.

Schena M. (2003). *Microarray Analysis*. John Wiley & Sons, Inc.: Hoboken, Canada.

Shinoda Y, Sakai Y, Uenishi H, Uchihashi Y, Hiraishi A, Yukawa H *et al.* (2004). Aerobic and anaerobic toluene degradation by a newly isolated denitrifying bacterium, *Thauera* sp. strain DNT-1. *Appl Environ Microbiol* **70**: 1385–1392.

Stralis-Pavese N, Sessitsch A, Weilharter A, Reichenauer T, Riesing J, Csontos J *et al.* (2004). Optimization of diagnostic microarray for application in analysing landfill methanotroph communities under different plant covers. *Environ Microbiol* **6**: 347–363.

Tarlera S, Denner EB. (2003). *Sterolibacterium denitrificans* gen. nov., sp. nov., a novel cholesterol-oxidizing, denitrifying member of the beta-Proteobacteria. *Int J Syst Evol Microbiol* **53**: 1085–1091.

Thomsen TR, Kong Y, Nielsen PH. (2007). Ecophysiology of abundant denitrifying bacteria in activated sludge. *FEMS Microbiol Ecol* **60**: 370–382.

Tsuneda S, Miyauchi R, Ohno T, Hirata A. (2005). Characterization of denitrifying polyphosphate-accumulating organisms in activated sludge based on nitrite reductase gene. *J Biosci Bioeng* **99**: 403–407.

Wagner M. (2009). Single cell ecophysiology of microbes as revealed by Raman microspectroscopy or secondary ion mass spectrometry Imaging. *Annu Rev Microbiol* (e-pub ahead of print 10 June 2009) PMID: 19514853.

Wagner M, Nielsen PH, Loy A, Nielsen JL, Daims H. (2006). Linking microbial community structure with function: fluorescence *in situ* hybridization-microautoradiography and isotope arrays. *Curr Opin Biotechnol* **17**: 1–9.

Whiteley AS, Manefield M, Lueders T. (2006). Unlocking the 'microbial black box' using RNA-based stable isotope probing technologies. *Curr Opin Biotechnol* **17**: 67–71.

Wilson KH, Wilson WJ, Radosevich JL, DeSantis TZ, Viswanathan VS, Kuczmarski TA *et al.* (2002). High-density microarray of small-subunit ribosomal DNA probes. *Appl Environ Microbiol* **68**: 2535–2541.

Yilmaz LS, Noguera DR. (2004). Mechanistic approach to the problem of hybridization efficiency in fluorescent *in situ* hybridization. *Appl Environ Microbiol* **70**: 7126–7139.

Zeng RJ, Saunders AM, Yuan Z, Blackall LL, Keller J. (2003). Identification and comparison of aerobic and denitrifying polyphosphate-accumulating organisms. *Biotechnol Bioeng* **83**: 140–148.

Zhou J. (2003). Microarrays for bacterial detection and microbial community analysis. *Curr Opin Microbiol* **6**: 288–294.